

Near-Field Tsunami Characteristics of Giant Earthquakes in Chile (1960), Alaska (1964), and Sumatra (2004)

George Plafker and J.C. Savage (U.S. Geological Survey, Menlo Park, CA)

INTRODUCTION

The Mw 9.5 Chile earthquake sequence (21-22/05/1960), the largest instrumentally recorded seismic event in history, was generated by a megathrust rupture of the southern end of the Peru-Chile Arc about 850 km long and 60–150 km wide down dip. Within Chile, the accompanying tsunami, to 15 m high, took an estimated 1,000 of the more than 2,000 lives lost due to the earthquake. The trans-Pacific tsunami killed 230 people in Japan, Hawaii and the Philippine Islands. The tsunami source was primarily regional offshore up warp with possible superimposed larger local uplift due to displacement on splay faults.

The Mw 9.2 Alaska earthquake (27/03/1964) ruptured major segments of the eastern Aleutian Arc 800 km long by 250–350 km wide down dip. Coseismic uplift along splay faults offshore generated a major near-field tsunami to 13 m high in Alaska that took at least 21 lives and local waves generated by submarine landslides in fords within Prince William Sound generated local waves with run up to 52 m that took about 77 lives. In addition, tectonically-generated tsunami waves were generated over the continental shelf and slope due to regional uplift that averaged 2-4 m; these waves added to the damage in Alaska, and they caused 15 deaths and local property damage as far away as Oregon and California.

The Mw 9.15 Sumatra earthquake (26/12/2004) ruptured segments of the Sunda Arc 1200+ km long by 150–200 km wide down dip. The accompanying near-field tsunami runup was as much as 36+ m in northern Sumatra where it caused 169,000 casualties along 200 km of shoreline and the far-field tsunami took an additional 63,000 lives throughout the Indian Ocean region; the deadliest tsunami in recorded history. In addition to the regional uplift by slip on the megathrust, major coseismic splay fault source(s) are inferred within the forearc from intraplate seismicity, and the tsunami arrival times, heights, and periods as recorded on the north Sumatra coast.

Data for all three giant earthquakes show that near-field tsunamis caused 73% of the deaths and most of the damage due to the combination of slip on intraplate splay faults that break relatively steeply to the surface (Alaska, Sumatra, and Chile?), regional up-dip slip on the megathrust, and by submarine slides along steep-sided fords (Alaska and Chile?). Near-field wave sources are especially hazardous because the initial wave at the source can be higher and closer to shore than for slip entirely on the megathrust. As a result, warning time to inhabitants can be significantly decreased and property damage is increased.

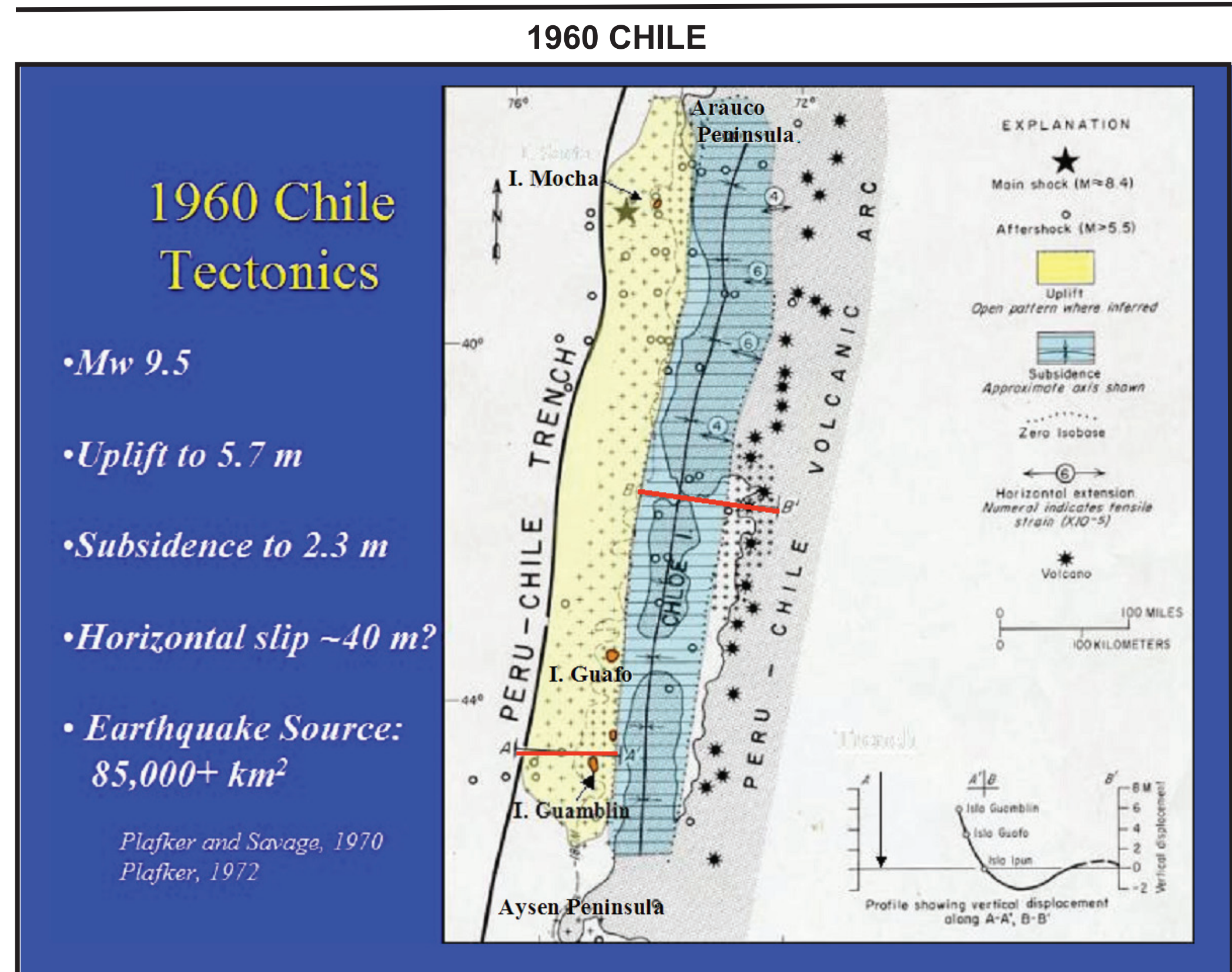


Figure 1. Regional coseismic surface displacements that between the Chile Trench and volcanic arc included ~170,000 km². Coseismic vertical displacements are characterized by a broad asymmetric downwarp to as much as -2.3 m between the mainland coast and the volcanic arc and a contiguous zone of upward to as much as 5.8 m that includes part of the Arauco Peninsula on the mainland coast and several offshore islands. Aftershock distribution suggests that the zone of uplift extends seaward to the Chile Trench. Dislocation models of the vertical surface displacements and seismic data indicate average and maximum megathrust slip was about 20 m and 54 m, respectively, and average landward dip is estimated at ~10°.

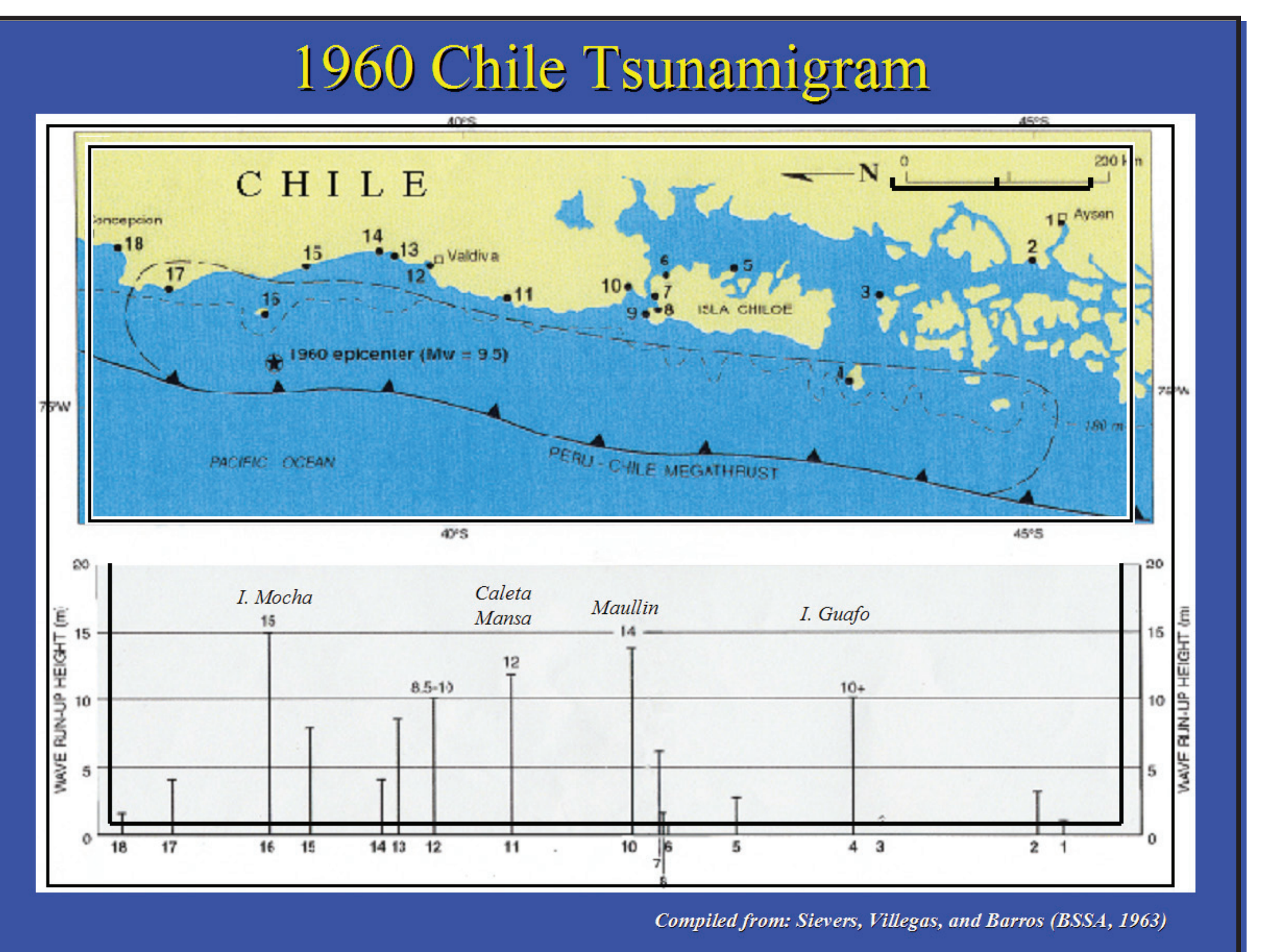


Figure 2. Coseismic offshore vertical displacements generated a near-field tsunami with regional run up of 4-12 m and peak run up of about 15 m along the outer coast of Chile. It also generated the largest and most destructive trans-Pacific tsunamis of modern times.

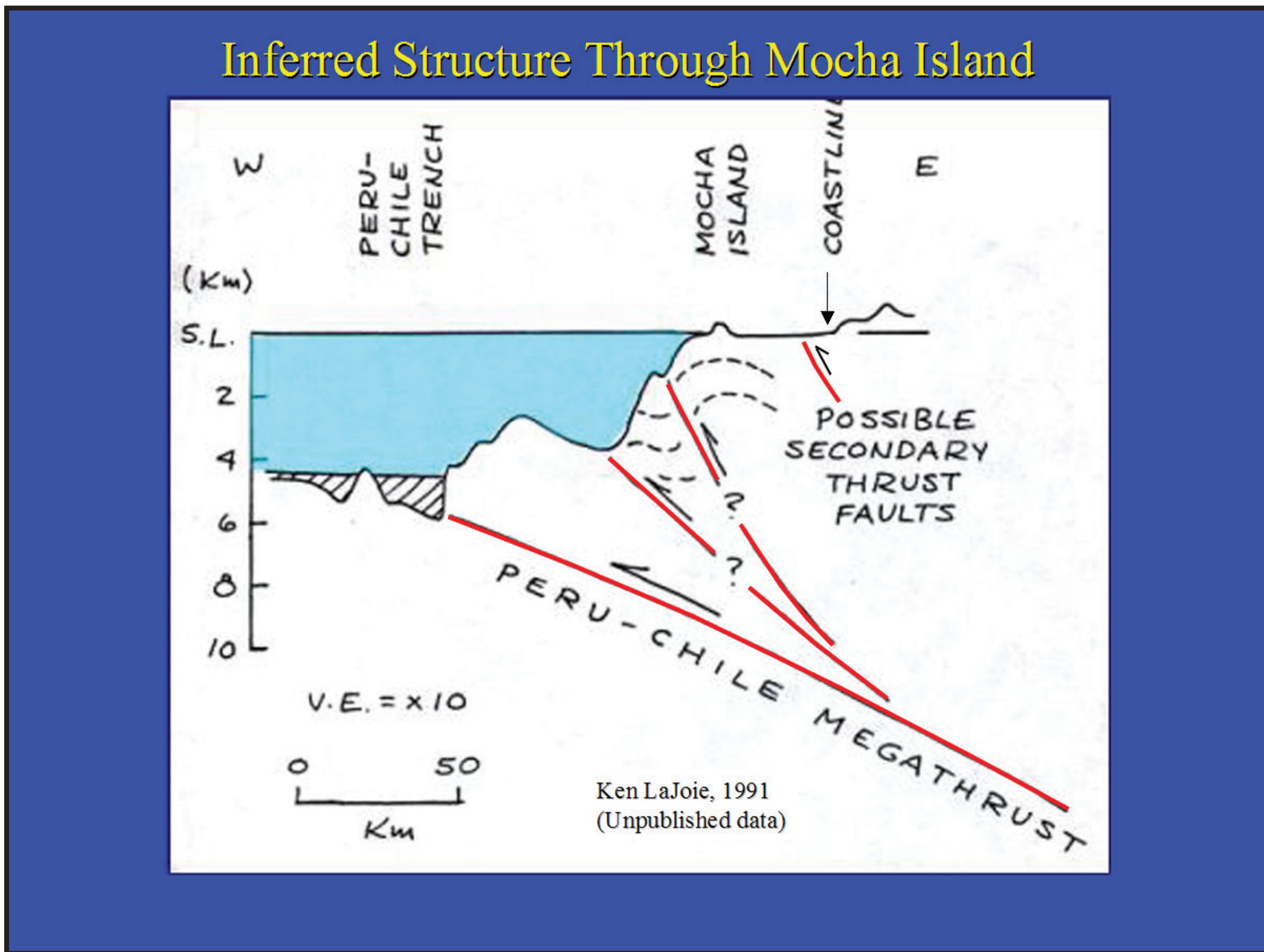


Figure 3. At Isla Mocha (see Fig. 1 for locations) the direction and timing of waves with the highest reported runup (~15 m), together with surface geology and seismicity are suggestive of one or more local intraplate splay fault sources at or near the edge of the continental shelf that are superimposed on the overall broad upward due to megathrust slip at depth. Similar splay faulting is suggested by dislocation models of vertical displacements in the southern part of the source region (Fig. 1, profiles A-A' and B-B').

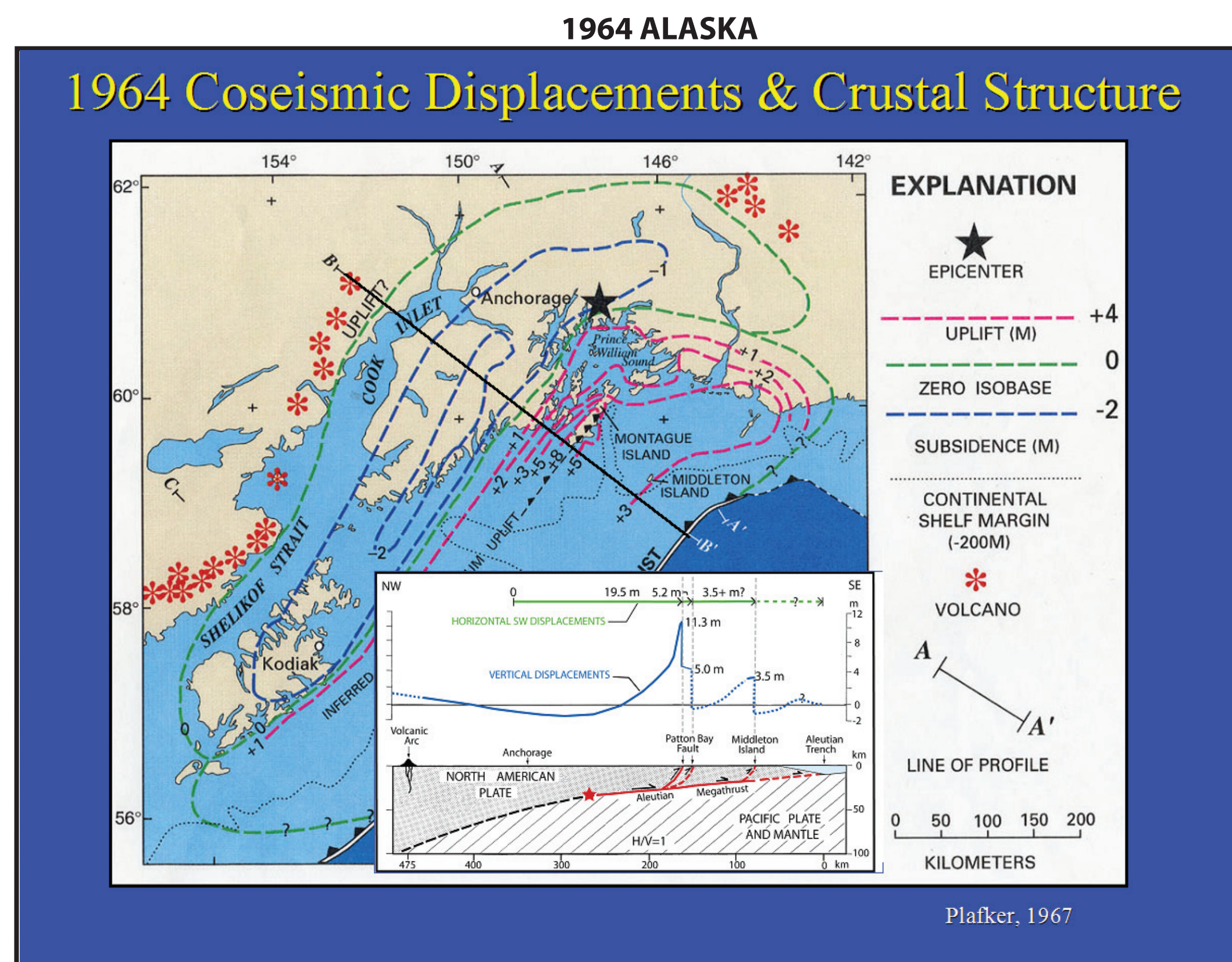


Figure 4. Regional coseismic surface displacements between the Aleutian Trench and volcanic arc included more than 140,000+ km². Coseismic vertical displacements are characterized by a broad asymmetric downwarp to as much as -2.3 m between the mainland coast and the volcanic arc and a contiguous zone of upward that averages about 2 m and locally is as much as 11+ m that includes much of Prince William Sound and the continental shelf and offshore islands. Major coseismic splay faults at and near Montague I. and Middleton I. were involved in uplift and tsunami generation in the forearc.

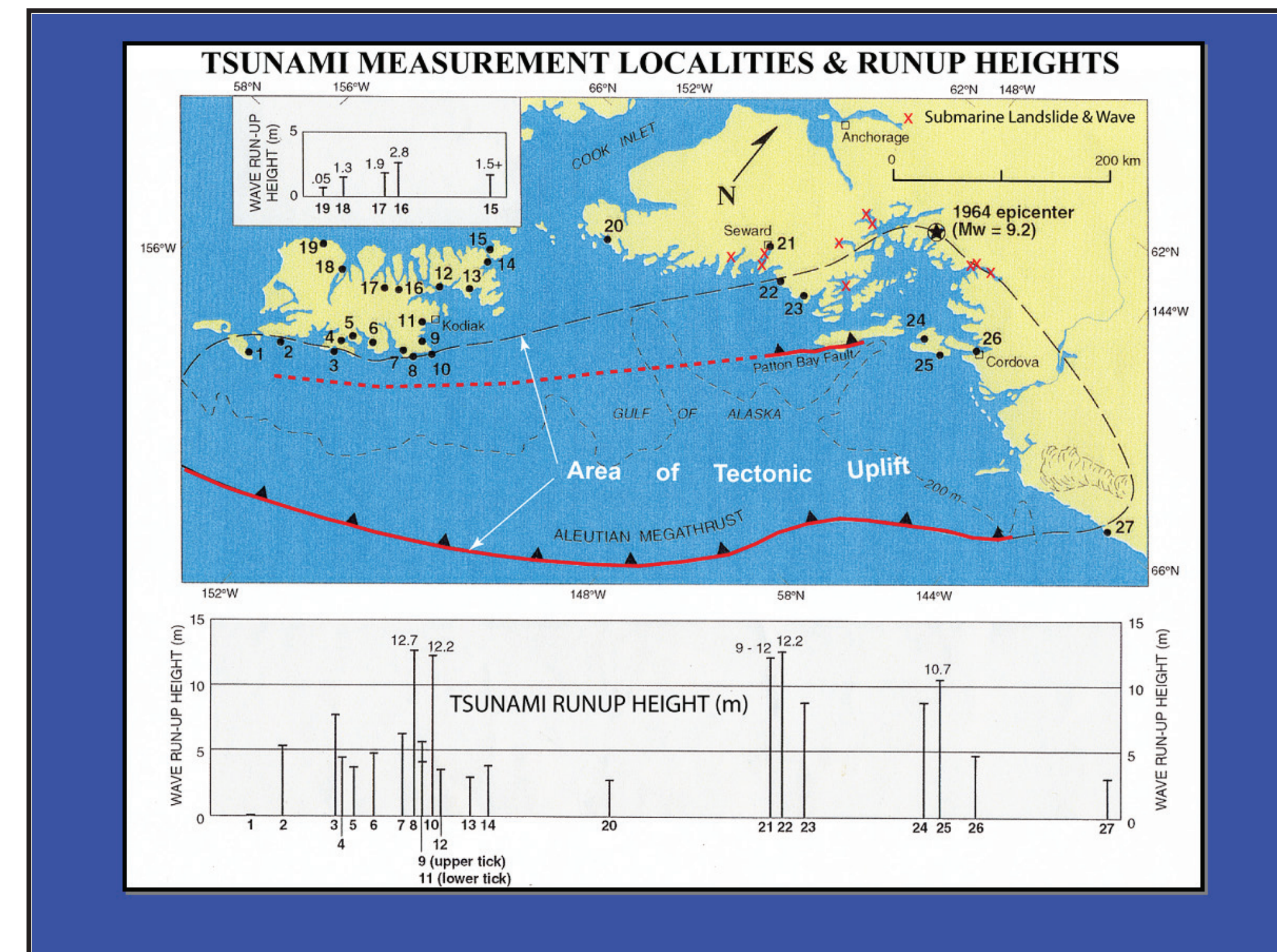


Figure 5. Coseismic offshore vertical displacements generated a near-field tsunami with regional run up of 4-10 m along the outer coast of Alaska and local maxima of as much as 12.7 m. Waves caused by earthquake-triggered submarine landslides in areas of steep submarine topography in Prince William Sound and near Seward (red 'x's) resulted in local extreme wave heights to a maximum elevation of 52 m. According to eyewitnesses, most of these slide-generated waves impacted shorelines during, or within minutes after, the earthquake.

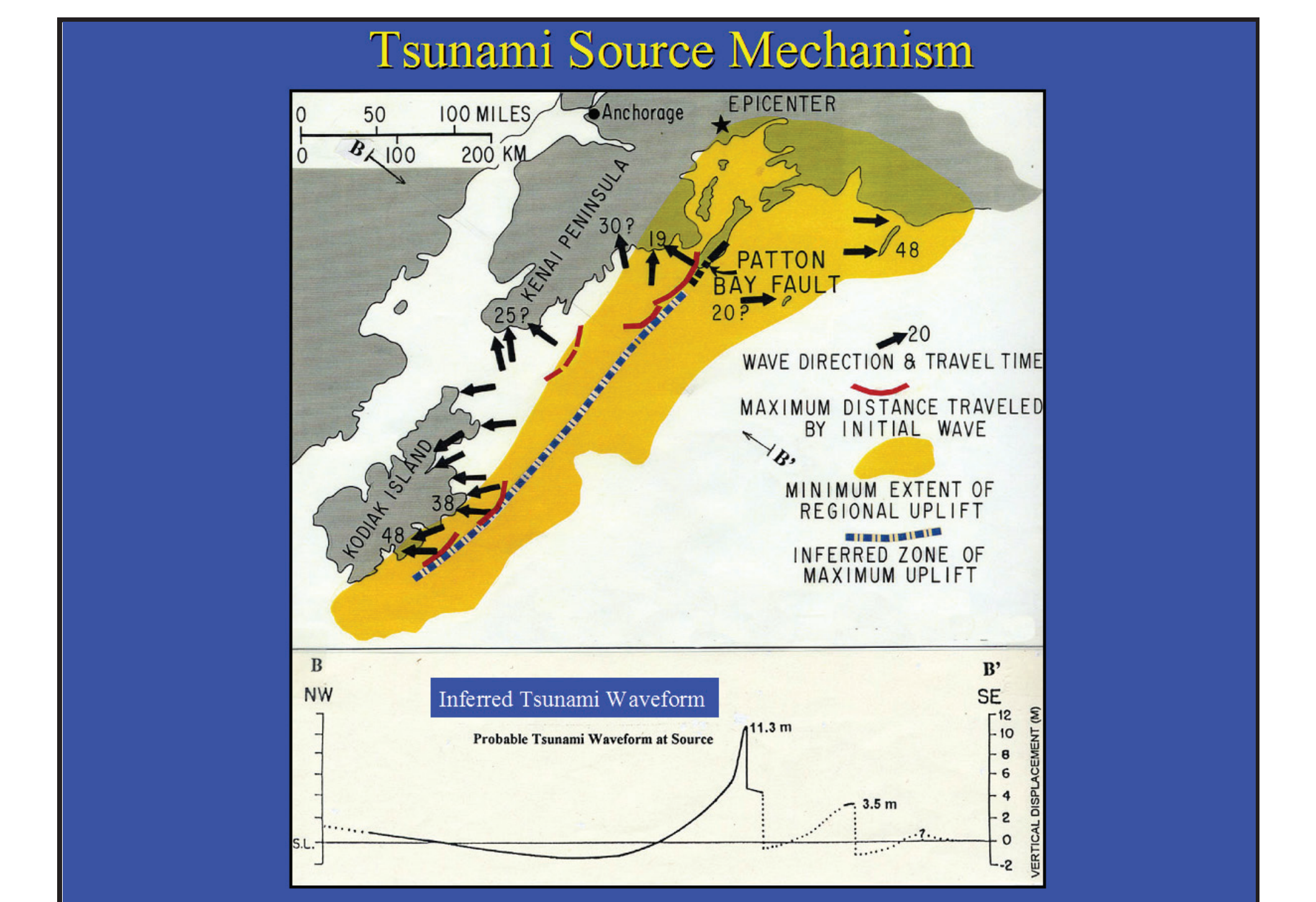


Figure 6. Tsunami travel directions and arrival times along the outer coast suggest a near-field high amplitude source mechanism inferred to be mainly related to 11-m uplift along the Patton Bay fault and its inferred offshore extension to the Kodiak Islands area. Regional uplift (yellow area) also generated a low-amplitude, long-wavelength tsunami in Alaska and caused damage and 15 deaths at sites along the NW Pacific Ocean coast from British Columbia to northern California.

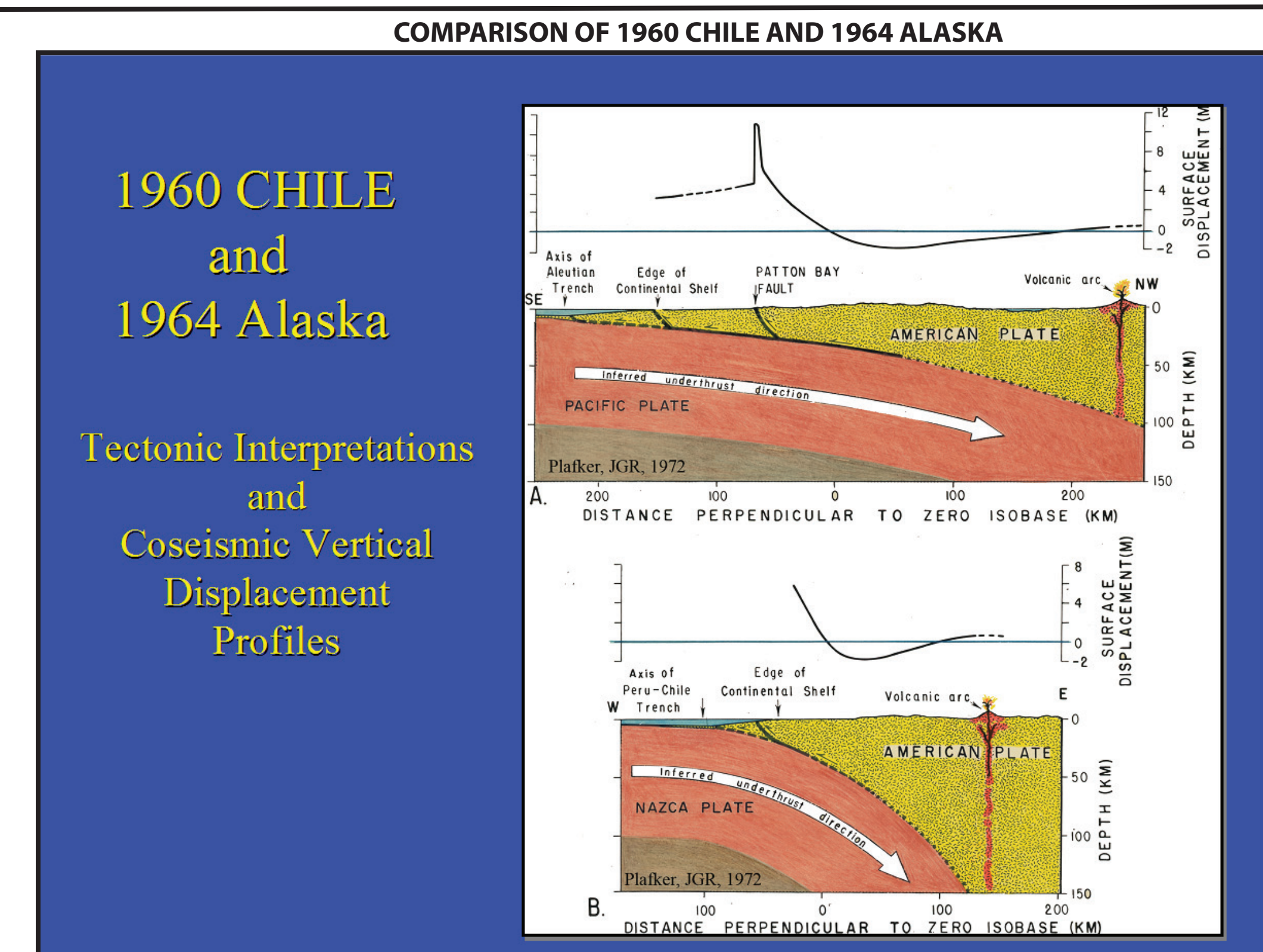


Figure 7. Schematic cross sections comparing suggested mechanisms for (A) the 1960 Chile earthquake (Plafker and Savage, 1970) and (B) the 1964 Alaska earthquake (Plafker, 1965; 1969). Inferred faults are shown by solid lines and possible faults by dashed lines. Profiles of vertical displacements are the same as in Figures 1 and 4. The Alaska earthquake source differs significantly from Chile in that (1) it has a much wider forearc and shelf region (200+ km), (2) megathrust dip is much shallower (9° or less), and (3) calculated maximum slip of 20-30 m is less than 50% of Chile.

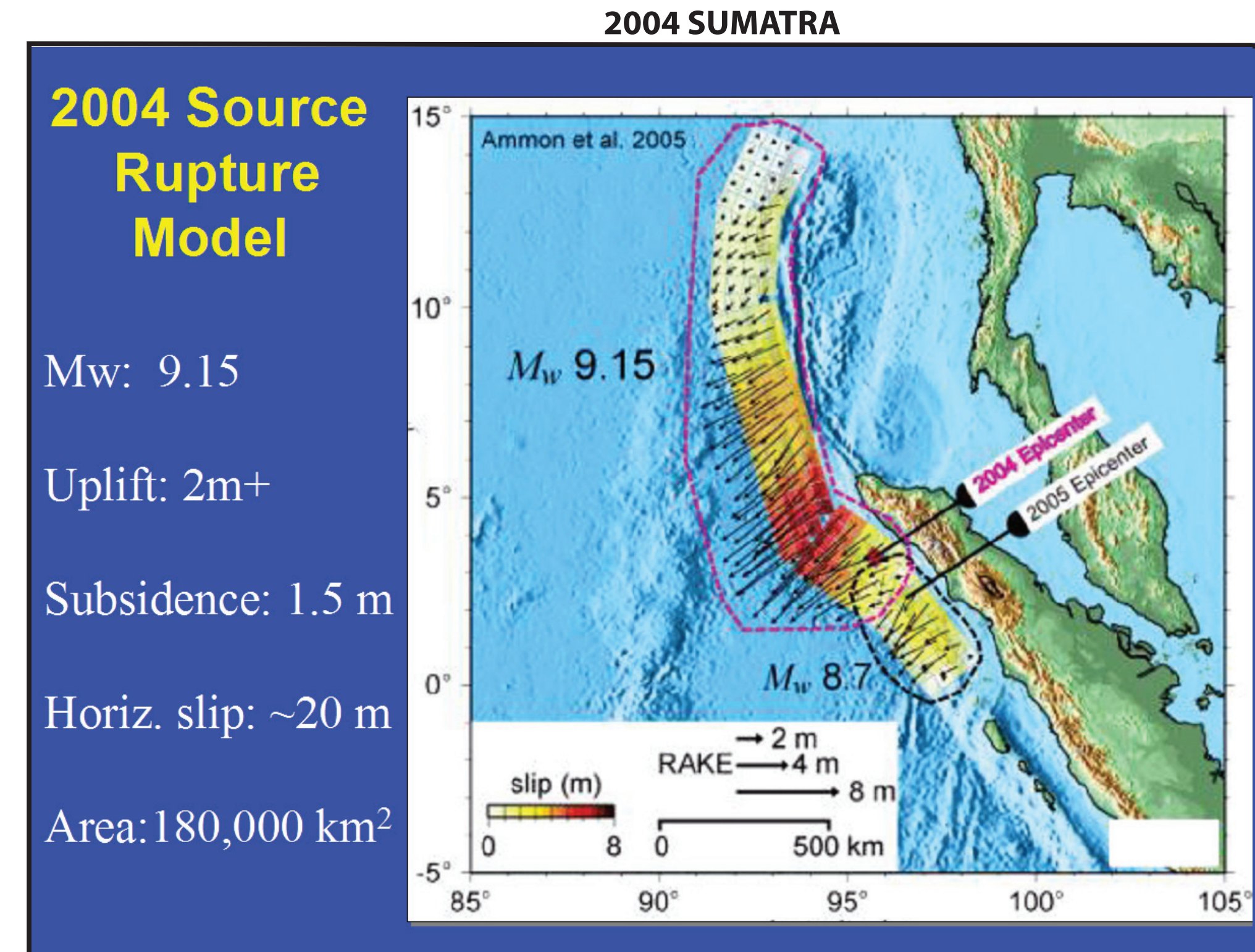


Figure 8. Seismic source data for the 2004 Sumatra earthquake indicate that coseismic deformation between the Sunda Trench and volcanic arc encompasses an area of about 180,000 km² (Ammon et al., 2005). Horizontal seismic slip offshore was as much as 20 m in the region off northern Sumatra and averaged ~10 m; slip diminished rapidly to the north and south. Regional subsidence to as much as 1.5 m occurred along the west coast of northern Sumatra. Because there are no offshore islands within the earthquake rupture region (except at the south end), direct observation of the vertical displacements in the outer rise could not be made in the area of maximum displacements. Seismic inversion data and megathrust dip suggest average uplift of less than 3 m in the region of maximum displacement offshore from northern Sumatra.

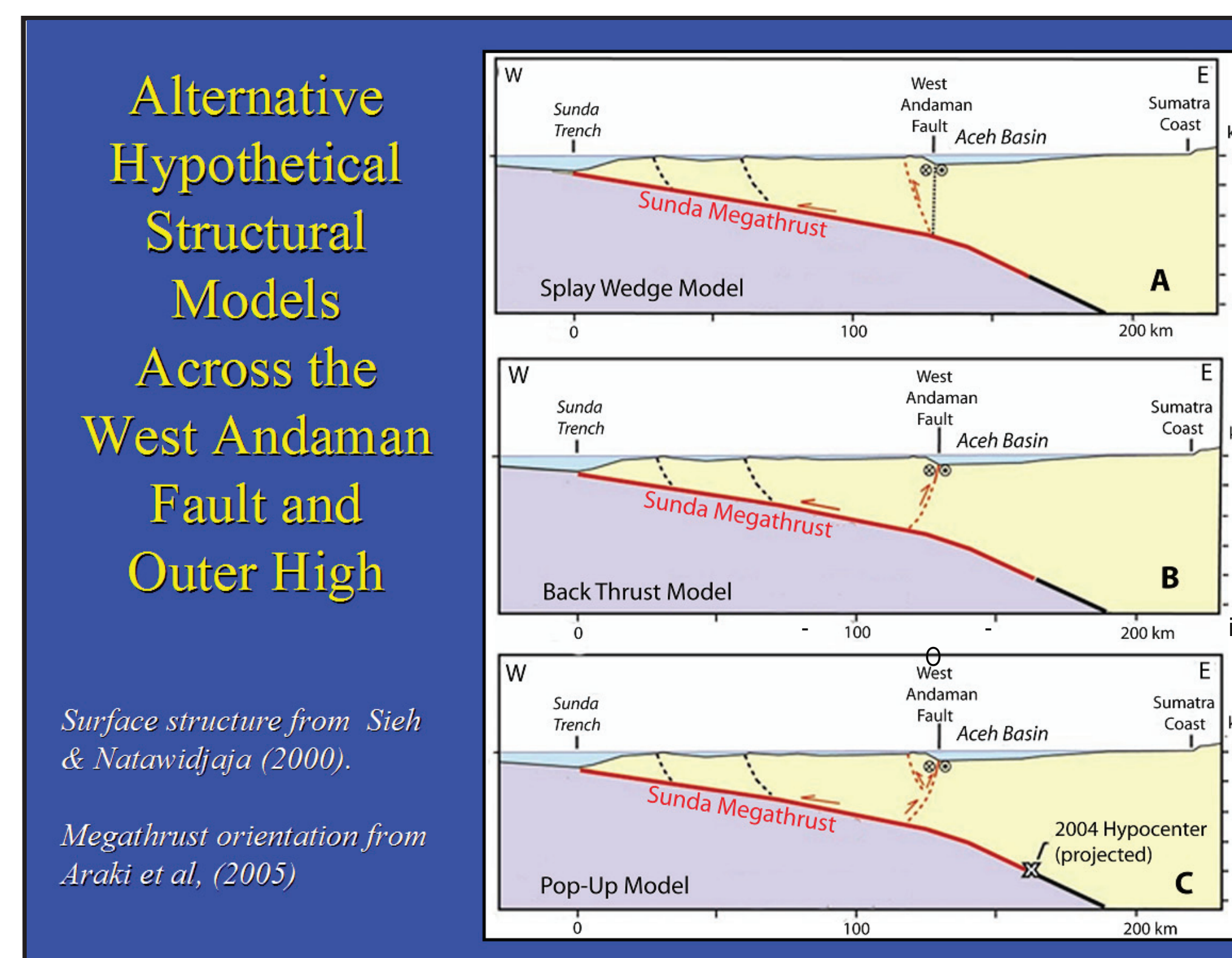


Figure 9. Alternative hypothetical structure models for an east-west section extending from the Sunda Trench across the outer high and Aceh Basin to the north tip of Sumatra. Faults shown are based on pre-2004 regional seismicity and topography by Sieh and Natawidjaja (2000), and post 2004 ocean bottom seismic surveys of aftershocks by Araki, et al. (2005).

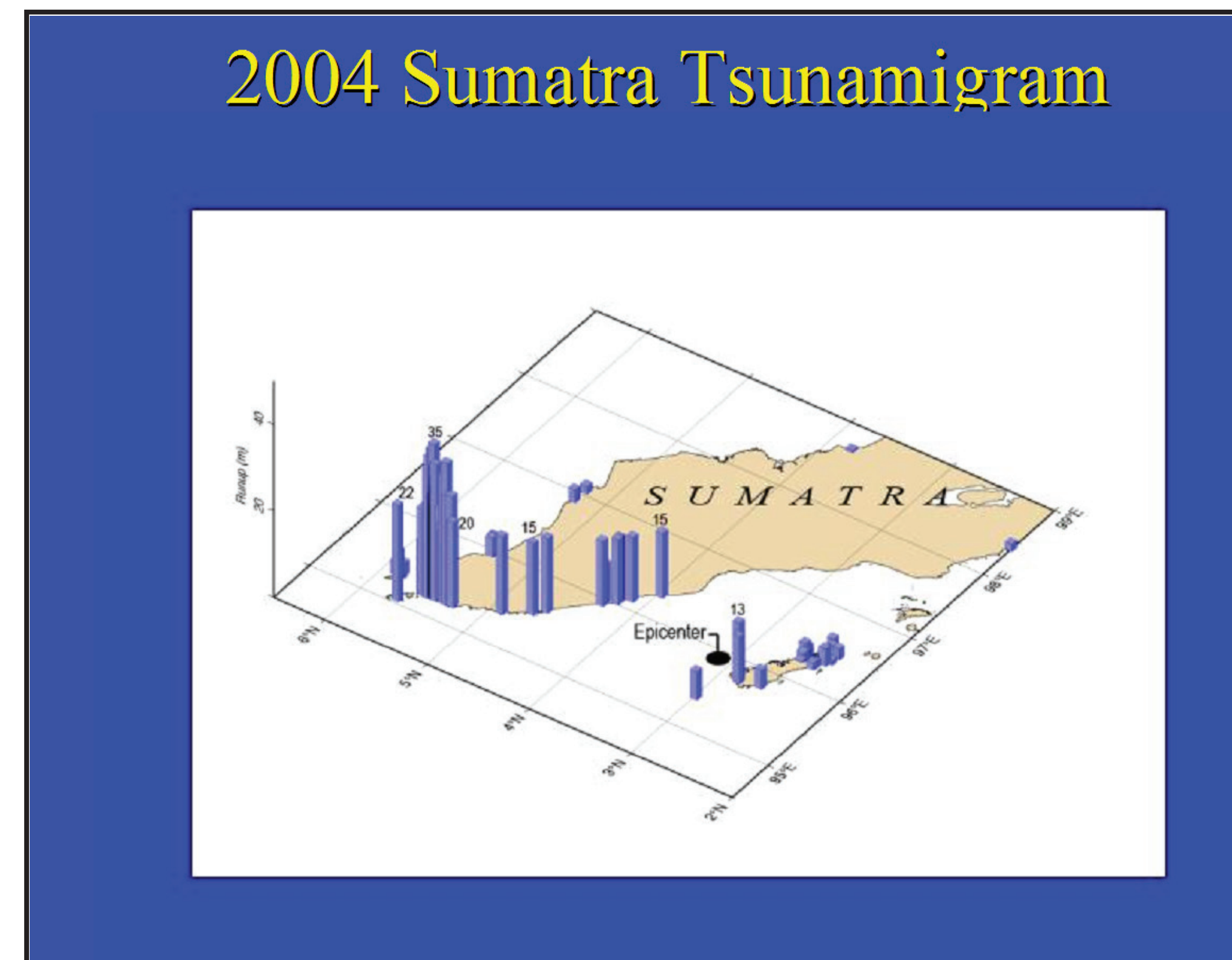


Figure 10. Tsunami runup heights of 15 to 35+ m along ~200 km of the northern Sumatra coast (Gerard Fryer, personal communication, 2008).

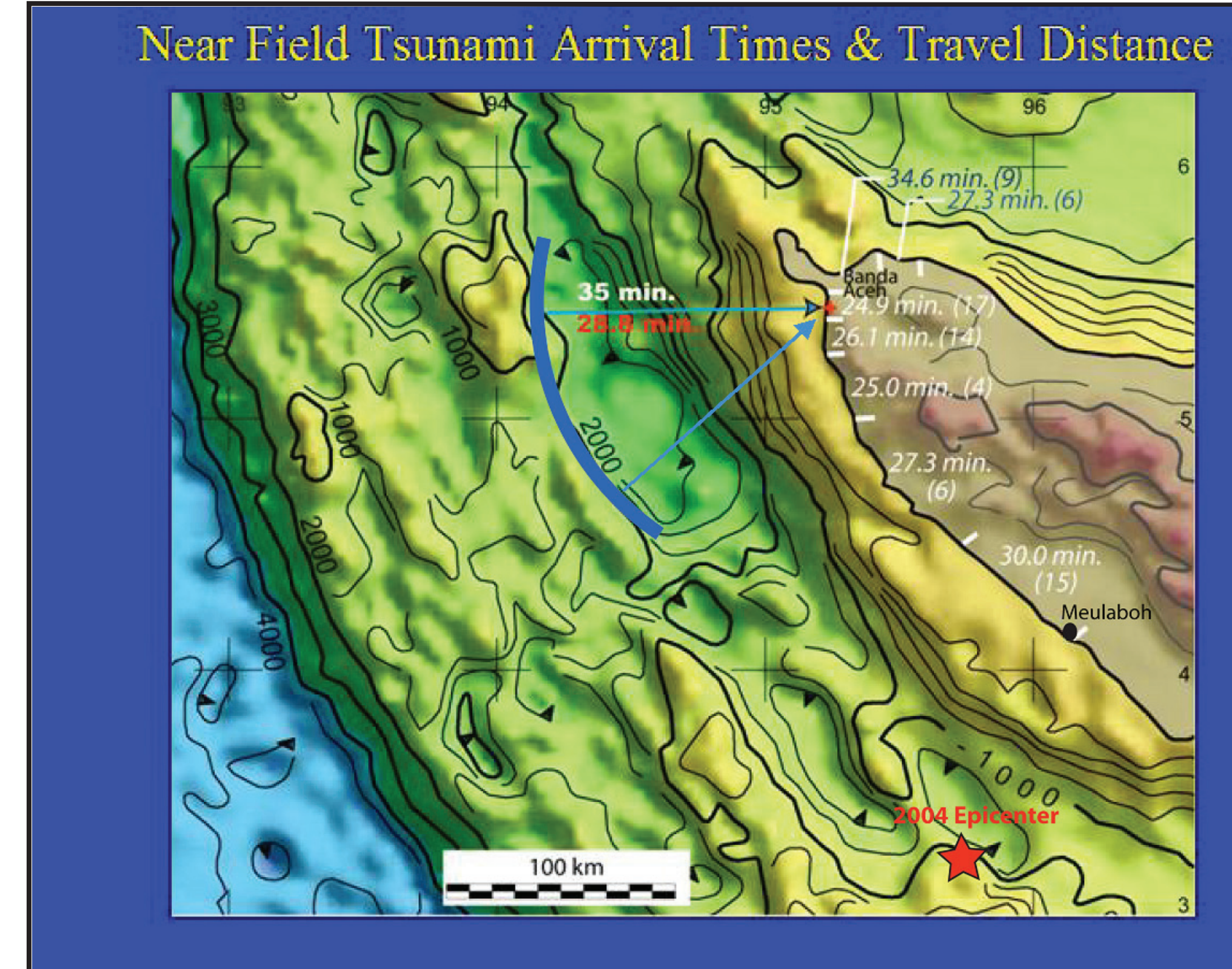


Figure 11. The most likely location of the source of the highest tsunami runup along the northern Sumatra coast is within the thick blue arc. The mean of 31 eyewitness accounts indicates that the earliest wave arrival was 25 to 26 minutes after start of the earthquake. The heavy blue arc represents a 29 to 35 minutes tsunami travel time, depending on assumptions about wave height at the source. The arrows show possible travel paths from two equidistant seismically active topographic highs that are interpreted as bounded on one or both sides by splay faults (see Fig. 9). Sources on the east side of the Aceh Basin seem to be precluded by marine survey data indicating absence of either recent faults or landslides capable of generating the extreme run up observed along the adjacent coast.

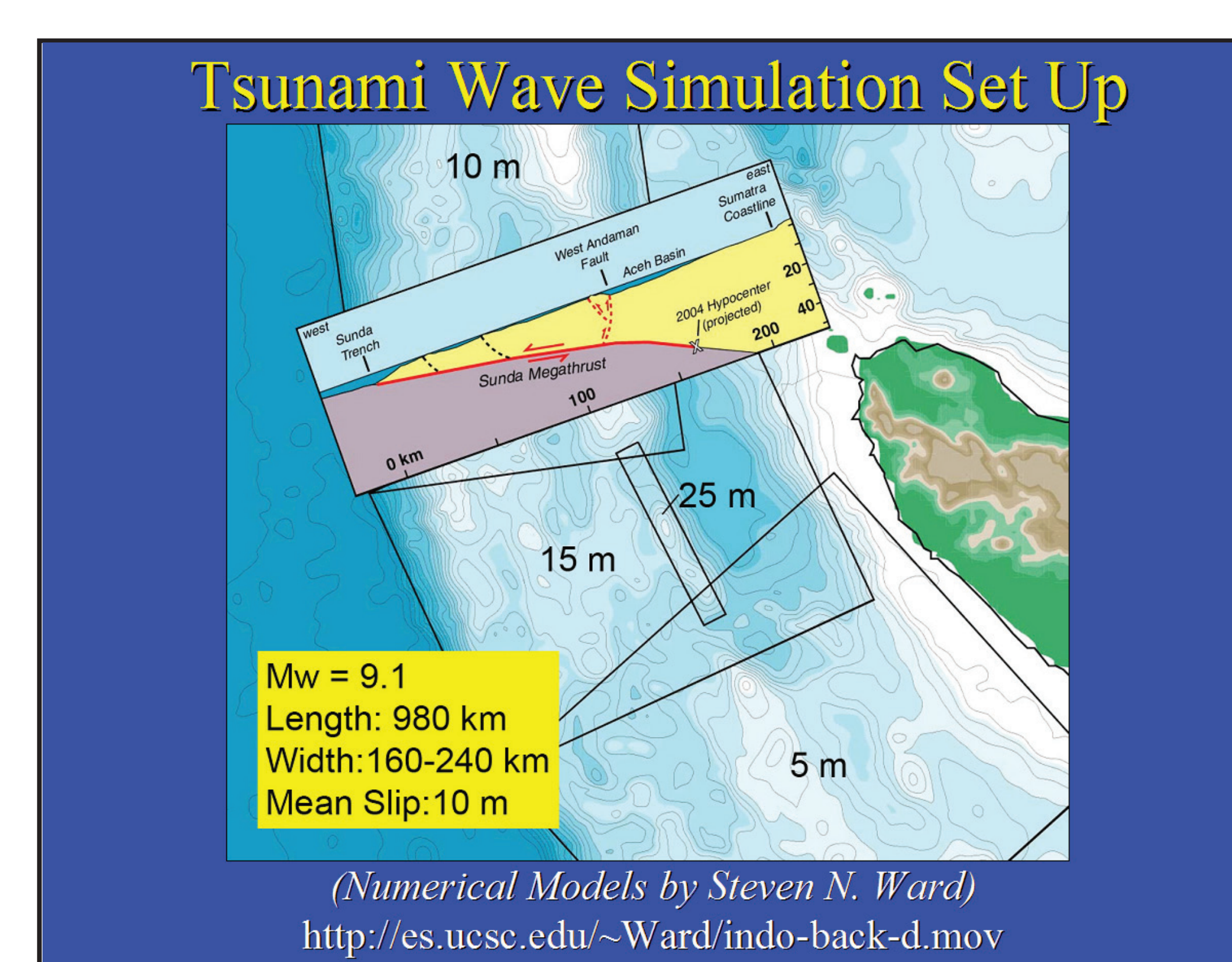


Figure 12. Set-up for a numerical model of the tsunami source off northern Sumatra assuming mean horizontal slip of 5-15 m on the Sunda megathrust (large boxes) and 25 m slip for a splay fault "pop-up" 100 km long at the west margin of the Aceh Basin (southern topographic high shown in Fig. 12). Structure section used for the model is one of three alternative splay fault configurations shown on Fig. 9-C. The tsunami wave simulation is in reasonable agreement with observed maximum wave heights and minimum arrival times along the NW Sumatra coast (Fig. 10) as well as the far-field wave train recorded at Phuket, Thailand (Ward, 2005).

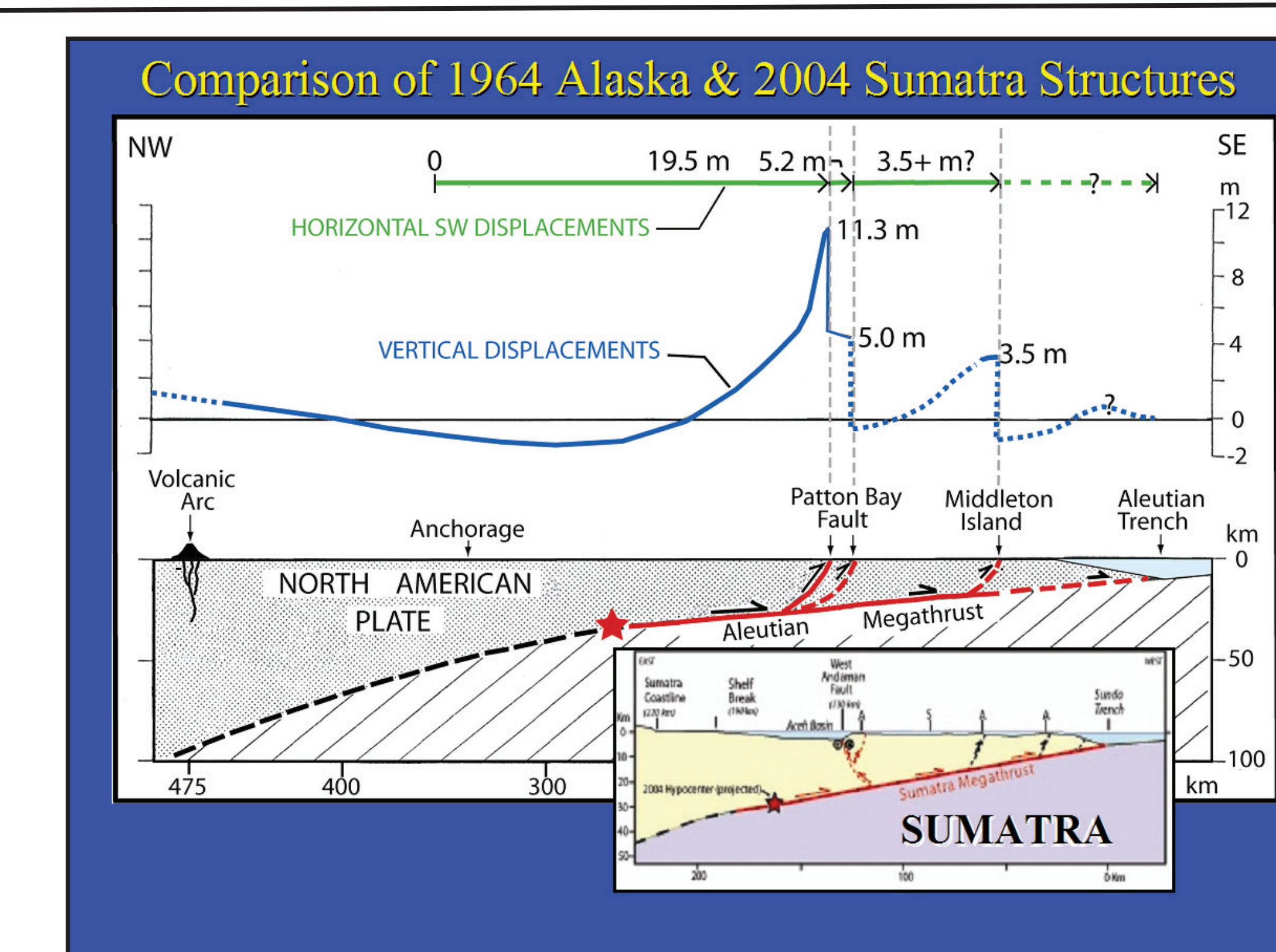


Figure 13. Structure sections across the eastern Aleutian Arc and Sunda Arc comparing the 1964 Aleutian megathrust and intraplate splay faults (Plafker, 1965) with the 2004 Sunda megathrust and probable intraplate splay faults based on topography, seismic activity, and marine geophysical data (Sieh and Natawidjaja, 2000; Araki, et al., 2005; Sibuet et al.). Sections are both at same scale. Note the shallow megathrust dips. The wide outer rises in both regions are composed largely of seaward-younging highly deformed accreted deep sea flysch and basaltic rocks. It is likely that some of the coseismic intraplate faults may be reactivating older structures within the accretionary prism.

COMPARISON OF FATALITIES FROM NEAR-FIELD AND FAR-FIELD TSUNAMIS	
1960 CHILE TOTAL	2,230+
Tsunami Near-Field	~1,000
Tsunami Far-Field	~230
1964 ALASKA TOTAL	129
Tsunami & Slide Waves Near-Field	~98
Tsunami Far-Field	~15
2004 SUMATRA TOTAL	232,000
Tsunami Near-Field	163,000
Tsunami Far-Field	63,000

Figure 14. Causes of fatalities from the three giant earthquakes

CONCLUSIONS

All three giant earthquakes show that the near-field tsunami hazards significantly exceed the hazard in the far-field (Figure 14).

A large part of the near-field hazard is a result of partitioning of total slip between the gently dipping megathrust and intraplate splay faults that break relatively steeply to the surface. For tsunami generation, this means that the initial wave at the source can be higher and closer to shore than it would be for slip entirely on the megathrust, thereby significantly increasing hazards to inhabitants and property on nearby shores.

Earthquake shaking in near-field areas of steep near-shore topography, such as fords and submarine canyons, may trigger local slide-generated waves with run up as high as 52 m that may impact shorelines during, or within minutes after, the earthquake.

More emphasis needs to be placed on delineating coasts subject to tsunamis from both intraplate faults and local slide-generated waves and on mitigation of their effects.

REFERENCES

Ammon, C.J., C. Ji, H.K. Thio, D. Robinson, S. Ni, V. Hjelvet, H. Kanamori, T. Lay, S. Das, D. Helmberger, G. Ichinose, J. Polet, D. Wald, Rupture Process of the 2004 Sumatra-Andaman Earthquake, *Science* 306 (2005) 1130-1139.
 Araki, E., M. Shinohara, K. Okana, T. Yamada, Y. Kaneda, T. Kanazawa, K. Suyetoro, Aftershock distribution of the 26 December 2004 Sumatra-Andaman earthquake from ocean bottom seismographic observation, *Earth, Planets and Space* 58 (2006) 115-119.
 Plafker, George, 1965. Tectonic deformation associated with the 1964 Alaska earthquake. *Science*, v. 148, p. 1675-1687.
 Plafker, George, 1969. Tectonics of the March 27, 1964, Alaska Earthquake. U.S. Geological Survey Professional Paper 543-I, 74 p.
 Plafker, George, and Savage, J.C., 1970. Mechanism of the Chilean earthquakes of May 21-22, 1960. *Geological Society of America Bulletin*, v. 81, p. 1001-1030.
 Plafker, George, 1972. The Alaskan earthquake of 1964 and Chilean earthquake of 1960: Implications for arc tectonics. *Journal of Geophysical Research*, v. 77, no. 5, p. 901-925.
 K. Sieh, D.H. Natawidjaja, Neotectonics of the Sumatran Fault, Indonesia, *J. Geophys. Res.* 105 (2000) 28,295-228,326.